Anomalous structural behavior and electronic structure in $ZrBe_2H_x$: Density functional calculations

D. J. Singh
Materials Science and Technology Division, Oak Ridge National Laboratory, Oak Ridge, Tennessee 37831-6032, USA

M. Gupta
Thermodynamique et Physico-Chimie d'Hydrures et Oxydes, EA3547, Batiment 415, Science des Materiaux, Universite Paris-Sud, 91405 Orsay, France

(Received 27 February 2007; revised manuscript received 19 June 2007; published 16 August 2007)

Density functional calculations are reported for $ZrBe_2$, $ZrBe_2H_2$, and supercells representing $ZrBe_2H_x$. We find that the H positions are soft in the sense that displacements along the hexagonal c axis are energetically favored for some orderings and displacement patterns. This is discussed in relation to the anomalous structural and nuclear magnetic resonance data reported for this compound. The mechanism for this softness is related to the electronic structure, specifically coupling to strongly hybridized bands occurring near the Fermi energy. In particular, certain patterns of H shifts along the c axis strongly mix H s and Zr d bands, leading to strong coupling between these shifts and bands at the Fermi energy and instabilities of phonons with these displacement patterns.

DOI: 10.1103/PhysRevB.76.075120 PACS number(s): 71.20.Be, 76.60.Gv

I. INTRODUCTION

$ZrBe_2H_x$ was reported by Maeland and Libowitz, who investigated various Be-based alloys in search for lightweight intermetallics suitable for hydrogen storage applications.[1–3] These hydrides form spontaneously and exothermically when the starting intermetallic, hexagonal AlB_2 (C32, $P6/mmm$) structure $ZrBe_2$, is exposed to hydrogen at room temperature and atmospheric pressure. This reaction forms a very stable hydride of composition $ZrBe_2H_{1.5}$ and decomposition plateau pressure below 0.1 kPa. A higher H content phase $ZrBe_2H_{2.3}$ can be formed using a hydrogen pressure of 13 MPa. The related compound $HfBe_2$ also forms a hydride but with a different H stoichiometry, $HfBe_2H$.[1,2]

Neutron scattering measurements showed that the hydride $ZrBe_2H_{1.5}$ maintains the same AlB_2 structure with expansion of the lattice and filling of triangular bipyramidal sites by H. Specifically, the hexagonal cell of $ZrBe_2$ (Fig. 1) has Zr and Be in sheets in the ab plane, Zr at (0,0,0), and Be at $(1/3,2/3,1/2)$ and $(2/3,1/3,1/2)$. According to the neutron refinement of Ref. 3, the H atoms in $ZrBe_2H_{1.5}$ then partially fill the open $2c$ sites, $(1/3,2/3,0)$ and $(2/3,1/3,0)$ in the Zr plane, so that each H is coordinated by three Zr at 2.14 Å in the plane and by two Be atoms, which form ···H-Be-H-Be··· chains with short 1.74 Å bond lengths along the c axis. Each H is coordinated in plane by three other nearest neighbor H sites at 2.14 Å.

However, the actual situation appears to be more complex. First of all, the volume expansion upon hydriding $ZrBe_2$ is remarkably small. There is a small 2.7% contraction of the in-plane a lattice parameter and a 7.3% expansion of c for a total volume expansion of only 1.8%, in contrast to the ~20% expansion often seen in intermetallic compounds and transition metals, corresponding to the usual range of 2–3 Å[3] volume increase per H. While the H-H distance is in accord with the Westlake criterion for stable hydrides, $d_{H\text{-}H} > 2.1$ Å,[4,5] the size of the hydrogen site is smaller than usual, leading to the suggestion that the $2c$ site is not the correct site.[6] Moreover, the difference between the Zr-H and Be-H distances in the ideal structure (0.40 Å) is significantly less than the difference in the Zr and Be covalent radii (0.58 Å). Secondly, powder neutron diffraction studies[7] of $ZrBe_2D_{1.5}$ find large displacement factors for D at 298 K and the continuous reversible development of weak superlattice peaks on cooling below ~250 K. While it was not possible to fully refine the structure including these peaks, it was noted that agreement was improved with models in which the D were randomly distributed among the tetrahedral $4h$ $BeZr_3$ sites, $(1/3,2/3,z)$, $z \sim 0.044$ at low temperature.

Nuclear magnetic resonance (NMR) studies of hydrogen diffusion in $ZrBe_2H_x$ were more consistent with two dimensional diffusion confined to the Zr plane (i.e., H on the $2c$ sites) than three dimensional motion based on modeling of the proton spin-lattice relaxation rate.[8,9] The activation energies extracted from these two dimensional hopping fits are consistent with quasielastic neutron scattering measurements at lower $x=0.56$.[10,11] NMR studies[12–14] also find a transition at ~235 K in $ZrBe_2D_x$ and at ~200 K in $ZrBe_2H_x$, $x \sim 1.5$,

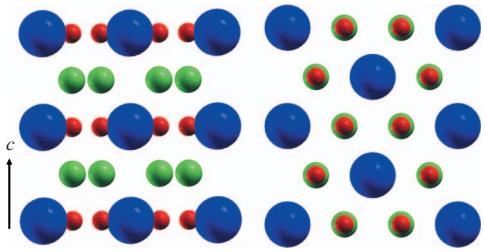

FIG. 1. (Color online) Structure of $ZrBe_2H_2$ as viewed along the a axis (left) and the c axis (right). The Zr are shown by the large blue spheres, Be by the medium green spheres, and H by the small red spheres. Note that the H lies in the Zr plane and forms linear chains of alternating H and Be along c. Figure 1 was prepared using the XCRYSDEN program (Ref. 33).

consistent with the temperature range where superlattice peaks develop in diffraction. This transition is characterized by the development of a large distribution of quadrupolar splittings reflecting a wide range of electric field gradients (EFGs) at the D sites.[13,14] This development of line broadening reflecting a range of D EFGs was surprising because a given type of site [$(2c)$ or $(4h)$] would normally be expected to show a narrower range even in a disordered material since the EFG reflects mainly the local environment.

Finally, it should be noted that $ZrBe_2$ is isostructural with MgB_2, which is a very high temperature conventional electron phonon mediated superconductor,[15–19] where superconductivity arises due to strong coupling of bond stretching phonons to holes in the bands associated with strong B–B σ bonds in the electron doped B sheets.[20–22] Similar but weaker bonds may be expected in electron doped Be sheets of the same structure, which may be the case in $ZrBe_2H_x$, since Be is more electronegative than Zr (Pauling electronegativity of 1.57 vs 1.33) and since H may contribute electrons to the valence bands. Charge transfers are often important in the formation of hydrides,[23–25] and this could potentially provide a framework for understanding the lattice effects in $ZrBe_2H_x$. It could also yield a rather interesting tunable material in which vibrational properties are a strong function of H content.

The purpose of the present paper is to elucidate the electronic structure and band formation in $ZrBe_2H_x$ in relation to $ZrBe_2$, and to investigate the issue of possible H displacements from the ideal $2c$ sites. We find that the H motions are coupled to hybridized Zr d_{xz}, d_{yz} bands near the Fermi energy and that this leads to instabilities and near instabilities against H displacements that are antisymmetric with respect to the Zr center.

II. METHOD

Here, we use density functional calculations to establish the electronic structure of $ZrBe_2H_x$ and to investigate the lattice stability with respect to H position. The calculations were done within the local density approximation (LDA) using the general potential linearized augmented plane wave (LAPW) method.[26] This method uses a flexible basis and makes no shape approximations to the potential or charge density. This makes it well suited for performing accurate density functional calculations for structurally complex materials. The calculations were based on the experimental lattice parameters, $a=3.716$ Å and $c=3.475$ Å, and LAPW sphere radii of $2.4a_0$, $1.5a_0$, and $1.0a_0$ for Zr, Be, and H, respectively. The calculations for nonhydrided $ZrBe_2$ were based on the lattice parameters, $a=3.817$ Å and $c=3.234$ Å, with all other parameters the same. We used well converged, tested Brillouin zone samplings and basis sets including local orbitals[27] to relax the linearization errors and to treat the semicore states of Zr. Specifically, we tested various zone samplings up to 576 special **k** points in the irreducible wedge of the hexagonal zone for $ZrBe_2H_2$ and $ZrBe_2$ and determined that a set of 80 **k** points yields converged results. All calculations shown used a grid at least this dense. The basis set consisted of more than 540 LAPW and local orbital functions for the primitive cell, and correspondingly larger values for the supercells. We also performed some calculations using the linear muffin-tin orbital method in order to determine the symmetries of states. However, all numerical results shown here are from the LAPW calculations.

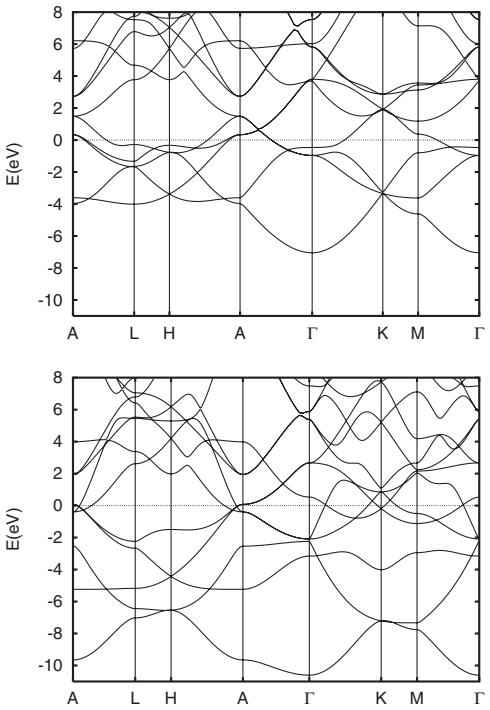

FIG. 2. Calculated band structures for $ZrBe_2$ (top) and $ZrBe_2H_2$ with H fully occupying the $2c$ sites (bottom). The Fermi level is at 0 eV.

III. ELECTRONIC STRUCTURE

The calculated band structures and corresponding electronic densities of states (DOSs) for the reference compounds, $ZrBe_2$ and $ZrBe_2H_2$, with H occupying all $2c$ sites are given in Figs. 2–4. The calculated energy difference between these two compounds in combination with the LDA energy of −2.294 Ry for the H_2 molecule[28] yields a formation energy of −156 kJ/mol H_2 for $ZrBe_2H_2$, consistent with the finding that $ZrBe_2H_x$ is a very stable hydride.

As may be seen from the DOS, both $ZrBe_2$ and $ZrBe_2H_2$ have strongly hybridized Be p–Zr d derived bands around the Fermi energy. This is markedly different from MgB_2 where the states near E_F are predominantly B derived with little involvement of Mg.[21] Qualitatively similar to MgB_2, the lowest valence bands below ~−3.5 eV in $ZrBe_2$ have Be s character. The higher valence bands up to E_F have hybridized Zr d–Be p σ–H s character. The doubly degenerate σ bands in $ZrBe_2$ have much more dispersion along the c-axis direction than in MgB_2 and, as a result, cross E_F along the Γ-A line. The three dimensionality of the band structure for the σ bands is quite different from MgB_2 and reflects hybridization with Zr. Introducing H leads to the introduction of H s derived states below the Fermi energy, in particular, a dispersive band from ~−11 to −7 eV, which is primarily

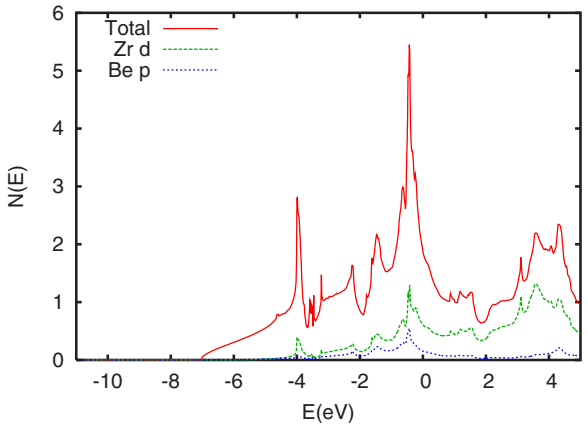

FIG. 3. (Color online) Calculated electronic DOS for $ZrBe_2$ and the Zr d and Be p projections onto the LAPW spheres. Note, however, that because of the small size of the Be sphere, much of the Be p projection strongly underestimates the importance of the Be contribution to the DOS. The DOS is on a per f.u. basis.

H s derived but hybridizes with the Be s-like band in the nonhydrided intermetallic, pushing the latter up in energy along the Γ-A line and leading to a relative sinking of the other valence bands with respect to the Fermi energy. This places E_F in the gap between the bonding and antibonding states in the hydride, with a large reduction in the DOS at E_F, $N(E_F)=0.22$ eV^{-1} for $ZrBe_2H_2$ vs $N(E_F)=1.88$ eV^{-1} for $ZrBe_2$, both on a per f.u. both spins basis. The values for the $x<2$ supercells were intermediate between those of $ZrBe_2$ and $ZrBe_2H_2$.

IV. H OFF CENTERING

In order to address the question of the H positions in $ZrBe_2H_x$, we performed calculations for distortions of the ideal $ZrBe_2H_2$ structure, as well as for various supercells with different H vacancy ordering patterns. We begin with the results for $ZrBe_2H_2$ with no H vacancies.

Total energy calculations as a function of H position away from the Zr plane showed that $ZrBe_2H_2$ is unstable against H

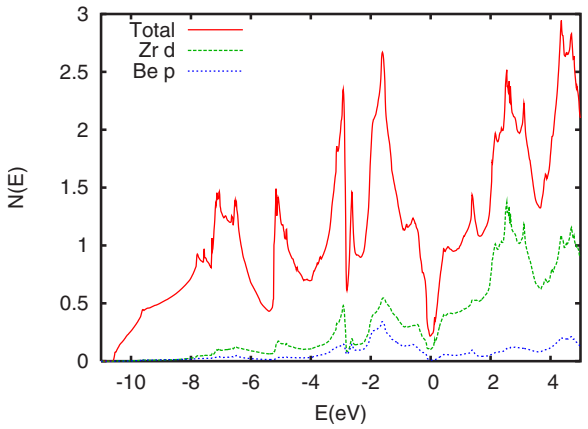

FIG. 4. (Color online) Calculated electronic DOS for $ZrBe_2H_2$ with H in all 2c sites. Projections of Zr d and Be p characters are also shown.

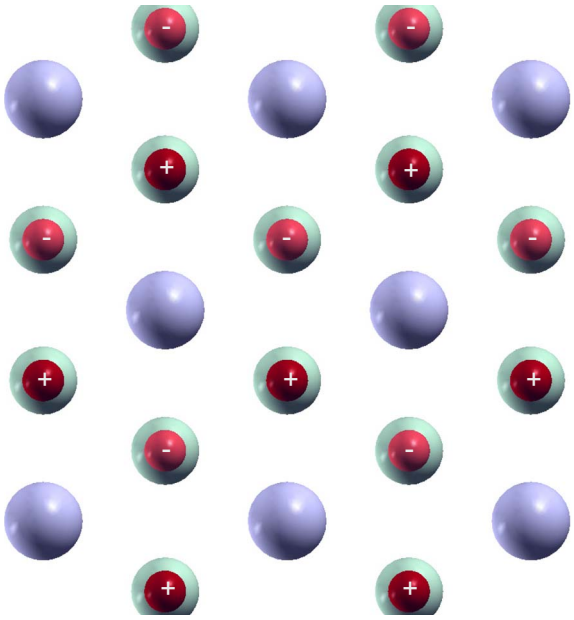

FIG. 5. (Color online) Distortion pattern A. The H moving up and down are shown by the small dark and light red spheres, with + and − signs, respectively.

displacement toward the 4h sites, but that the instability depends on the pattern of off centering and H vacancy ordering. In particular, if both H in the unit cell are displaced in the same direction (this distortion is denoted "S" in the following) the energy increases, while if one is displaced in the $+z$ direction and the other by the same amount in the $-z$ direction (denoted "A"), the energy decreases. From a nearest neighbor point of view, in the former mode, all H have H nearest neighbors displacing in the same direction, while in the latter, the three neighboring H move in the opposite direction, as shown in Fig. 5. Both of these distortions correspond to dimerizations of the ···Be-H-Be-H··· chains. The calculated energy minimum, −1.6 mRy/cell lower than the undistorted structure, was at a H displacement of 0.19 Å away from the Zr planes with pattern A. This is more than twice the distance to the ideal centers of the tetrahedral sites as defined by Westlake.[6]

The fully relaxed structure, allowing shifts of the metal atoms as well, had Zr at its symmetric site (0,0,0), shifts of the H in the c-axis direction of 0.17 Å, and much smaller shifts along c of the Be opposite to the H in a given c-axis chain, by 0.01 Å. These opposite shifts of Be and H might suggest a tendency toward dimerization of the chains or distortion of the Be sheets, perhaps related to what was observed in $SrAl_2H_2$, where sp^3 hybridization was found to be important.[29] However, in that case, the ratio of Al to H shifts is ~−0.42, as compared to the much smaller ratio of Be to H shifts of ~−0.07 in the present case.

It should be emphasized that both unstable A and S distortion patterns involve low energies. The S distortion where both H move together has a harmonic vibrational frequency of 550 cm^{-1}, which is very low for a H mode.[30]

The displacement with unstable pattern A is accompanied by a distortion of the band structure near E_F, as shown in Fig. 6. In particular, bands near E_F around the zone center

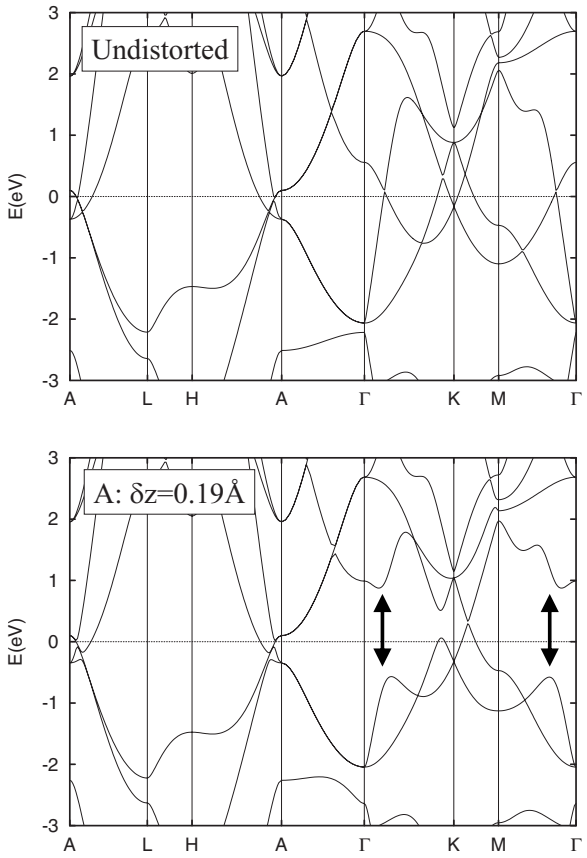

FIG. 6. Band structure near E_F for $ZrBe_2H_2$ with H in the $2c$ positions (top) and with the two H in the unit cell displaced along c by 0.19 Å in opposite directions (bottom). The gapped bands are highlighted by arrows in the lower panel.

are gapped away by ~0.7 eV for a 0.19 Å H displacement, which implies a rather large coupling for this band. Furthermore, because of the large energy range of this gapping for modest H displacement, it may be also expected to be effective for a range of H content, including $x=1.5$, since the Fermi energy still lies in the energy region affected by it. This is the case in the DOS for the "O" supercell, which is an $x=1.5$ supercell with 2 f.u., two of the three H moving oppositely and the third held at its symmetric position, as described below [not shown, $N(E_F)=0.93$ eV^{-1}/f.u.]. This gapping does not occur for stable distortion S. The strongly upward dispersing band along Γ-K and Γ-A, which forms the lower band in the pair that is gapped by the A distortion has, H s character at Γ and hybridizes with Zr d and Be p states away from Γ in the $k_z=0$ plane. The band that forms the downward dispersing member of the pair shows weaker k dependence and is of Zr d–Be p character. In a rhombohedral crystal field, the Zr d levels will split into a singly degenerate a_g orbital (d_{z^2}), which is fully symmetric with respect to rotation about the z axis, and four e symmetry orbitals in two crystal field split pairs, one of which is in plane (d_{xy},$d_{x^2-y^2}$) and the other is antisymmetric in the z reflection (d_{xz},d_{yz}). This latter group, which is the origin of the upper pair of bands that split with the A distortion, cannot hybridize with H s orbitals in the undistorted structure. Moving the H together above or below the plane (distortion S) does not lift this restriction, but antisymmetric A distortion, which has H atoms on opposite sides of the Zr moving in opposite directions, does. This leads to a mixing of the lower, H s derived band with the upper Zr derived band, and thus the opening of the gap.

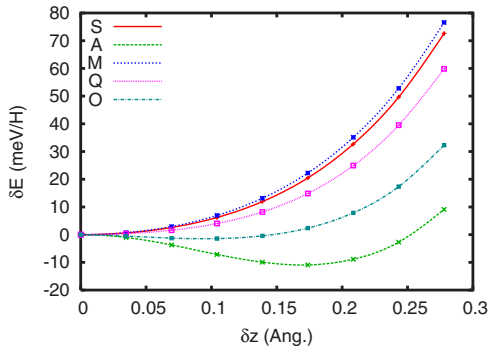

FIG. 7. (Color online) Energy as a function of H displacement, on a per displaced H basis, for the various supercells and displacement patterns (see text). All atoms other than H were fixed in their ideal positions. The energy zeros have been shifted so that the undistorted structures are at 0, although the different supercells have different cohesive energies.

We performed supercell calculations to relate our results more directly with experimental studies for $ZrBe_2H_x$, $x \sim 1.5$. These were the (1) primitive cell with one H removed ($x=1$, denoted "M"), (2) a cell doubled along c and containing chains of···H-Be-H-···with the H in each chain displaced in an alternating fashion along c but with all H in a given Zr plane displaced in the same direction ($x=2$, denoted "Q"), and (3) a doubled orthorhombic cell, $a_{orth}=a_{hex}$, $b_{orth}=b_{hex}+a^*_{hex}$, $c_{orth}=c_{hex}$, containing three H and one vacancy in which two of the H are displaced oppositely and the third left in the Zr plane ($x=1.5$, denoted "O"). Both of the $x<2$ supercells had lower energies per H (i.e., higher stability) than the ideal $x=2$ structure by 0.19 and 0.11 eV per H, for the $x=1$ (M) and $x=1.5$ (O) cells, respectively.[31] A qualitatively similar result was reported by Kodibagkar *et al.*, who considered more complex supercells.[12]

The energies of these supercells as a function of H distortion are given in Fig. 7. As may be seen, the softness of the H off centering depends on the environment. The two cases that have H on opposite sides of the Zr displacing in opposite directions (A and O) have the lowest energy for distortions. We note that the energy differences associated with varying H content are much larger than the scale associated with H displacement from the $2c$ sites. Thus, these displacements are not expected to play a role in the thermodynamics of hydrogen uptake.

V. ELECTRIC FIELD GRADIENTS

As mentioned, electric field gradients are sensitive probes of the local structure. The EFG is a rank 2 traceless tensor that derives from the quadrupole moments of the charge density and is directly measured via the Coulomb interaction with the nuclear quadrupole moments. In a uniaxial system, this tensor has one unique element, V_{zz}, while the in-plane

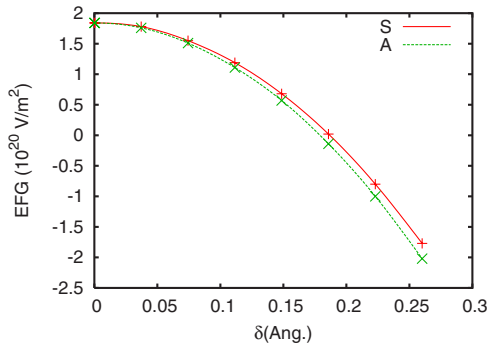

FIG. 8. (Color online) EFG V_{zz} for the H site in $ZrBe_2H_2$ as a function of displacement in patterns A and S (see text).

components are $V_{xx}=V_{yy}=-V_{zz}/2$. Figure 8 shows the calculated H EFG V_{zz} as a function of displacement in the A and S patterns for $ZrBe_2H_2$. As may be seen, the EFG is very sensitive to H displacements and in fact changes sign near the minimum energy for the A pattern. However, as is seen by comparing the A and S values, the EFG is not sensitive to the actual pattern of H displacements. Kodibagkar *et al.* extracted a motionally narrowed value $V_{zz}\sim 2\times 10^{19}$ V/m^2 for D in $ZrBe_2H_{1.4}$ at ambient temperature, with broadening and splitting of the quadrupole line at lower temperature, to a value of $V_{zz}\sim 2\times 10^{20}$ V/m^2.[12,13,32] This low temperature value is consistent with our calculated EFG if the majority of the H occupies the $2c$ sites at low temperature. It should also be noted that these are very small values for the EFG, indicating a nearly cubic site from the point of view of the field gradient. Based on our results, one may conjecture that the distribution of EFGs evident in the quadrupole line shapes may be due to disordered H displacements of ~0.1 Å, which would yield a distribution of EFG values that could fill in the spectrum between the two shoulders that may be identified as quadrupole peaks. However, while the EFG is not sensitive to the pattern of H displacements, it is sensitive to H vacancies. In the undistorted M cell ($x=1$), we obtain a H EFG $V_{zz}=0.51\times 10^{20}$ V/m^2, while in the O cell ($x=1.5$), we obtain a range from 0.85×10^{20} to 1.52×10^{20} V/m^2 for the different H sites, suggesting the more prosaic explanation that the line is narrowed at ambient temperature due to H motion and broadens as the H vacancies order. It may also be the case that the superlattice peaks observed in diffraction are related to (partial) H vacancy ordering. It will be of interest to perform more detailed structure refinements of $ZrBe_2H_2$ at low temperature using high flux neutron diffraction when this becomes possible.

VI. SUMMARY AND CONCLUSIONS

Density functional calculations for $ZrBe_2H_2$ reveal an electronic structure that has some features in common with MgB_2 but differs in the presence of strong hybdridization with Zr d states around the Fermi energy. Because of this, the σ bands, which are quite two dimensional in MgB_2, are three dimensional in $ZrBe_2H_2$. This strong involvement of Zr d states leads to strong coupling of bands near the Fermi energy with H positions. In particular, the coupling of d_{xz}, d_{yz} derived bands with H displacements along the c axis in patterns that are antisymmetric with respect to the Zr center is sufficiently strong to drive those modes to be unstable. This results in static displacements of the hydrogen away from the $2c$ sites. Since this instability requires a coordinated motion of more than one H, a more complex situation may be expected in $ZrBe_2H_x$, $x<2$, with weaker local off centerings depending on the local H vacancy environment. This might be expected to lead to a distribution of H displacements in the actual material. In fact, while the tendency to displace becomes weaker as the band filling is lowered from $x=2$, it still exists at $x=1.5$. With disordered H vacancies, only some of the Zr sites will have H atoms antisymmetrically placed around them so that opposing H displacements can occur. On the other hand, considering that the material has broad metallic bands and that the effective H-H interaction is apparently repulsive,[12] it is not expected that the effective band filling will vary much from site to site in actual samples. The net result is that weak shifts of the H away from the $2c$ sites with a wide distribution of magnitudes of the displacements relative to the size of the average displacement are expected. This may partially explain some of the anomalous neutron and NMR data on $ZrBe_2H_x$.

ACKNOWLEDGMENTS

The authors are grateful for helpful discussions with M. S. Conradi, V. D. Kodibagkar, and R. Gupta. The authors thank M. S. Conradi and V. D. Kodibagkar for a prepublication copy of their NMR data and the value of the D EFG obtained from it. D.J.S. thanks the University of Paris-Sud for the hospitality, which made this work possible. Work at ORNL was supported by DOE, EERE, FreedomCar and Vehicle Technologies Program. The authors thank the Institut du Developpement et des Ressources en Informatique Scientifique (IDRIS) for a grant of computer time.

[1] A. J. Maeland and G. G. Libowitz, J. Less-Common Met. **89**, 197 (1983).
[2] A. J. Maeland, J. Less-Common Met. **89**, 183 (1983).
[3] A. F. Andresen, K. Otnes, and A. J. Maeland, J. Less-Common Met. **89**, 201 (1983).
[4] D. G. Westlake, J. Less-Common Met. **90**, 251 (1983).
[5] D. G. Westlake, J. Less-Common Met. **91**, 275 (1983).
[6] D. G. Westlake, Mater. Res. Bull. **18**, 1409 (1983).
[7] B. C. Hauback, H. Fjellvag, and A. J. Maeland, J. Alloys Compd. **224**, 241 (1995).
[8] A. F. McDowell, C. F. Mendelsohn, M. S. Conradi, R. C. Bowman, Jr., and A. J. Maeland, Phys. Rev. B **51**, 6336 (1995).
[9] F. Kimmerle, G. Majer, U. Kaess, A. J. Maeland, M. S. Conradi, and A. F. McDowell, J. Alloys Compd. **264**, 63 (1998).

[10] R. L. Cappelletti, Z. Chowdhuri, T. J. Udovic, R. M. Dimeo, B. C. Hauback, and A. J. Maeland, Phys. Rev. B **73**, 224109 (2006).
[11] R. L. Cappelletti, T. J. Udovic, Z. Chowdhuri, B. C. Hauback, A. J. Maeland, and R. M. Dimeo, Physica B **385-386**, 208 (2006).
[12] V. D. Kodibagkar, P. A. Fedders, C. D. Browning, R. C. Bowman, Jr., N. N. Adolphi, and M. S. Conradi, Phys. Rev. B **67**, 045107 (2003).
[13] V. Kodibagkar, J. L. Herberg, R. C. Bowman, Jr., and M. S. Conradi, J. Alloys Compd. **330-332**, 179 (2002).
[14] V. D. Kodibagkar, C. D. Browning, X. Tang, Y. Wu, R. C. Bowman, Jr., and M. S. Conradi, Solid State Nucl. Magn. Reson. **24**, 254 (2003).
[15] J. Nagamatsu, N. Nakagawa, T. Muranaka, Y. Zenitani, and J. Akimitsu, Nature (London) **410**, 63 (2001).
[16] G. Karapetrov, M. Iavarone, W. K. Kwok, G. W. Crabtree, and D. G. Hinks, Phys. Rev. Lett. **86**, 4374 (2001).
[17] T. Takahashi, T. Sato, S. Souma, T. Muranaka, and J. Akimitsu, Phys. Rev. Lett. **86**, 4915 (2001).
[18] S. L. Bud'ko, G. Lapertot, C. Petrovic, C. E. Cunningham, N. Anderson, and P. C. Canfield, Phys. Rev. Lett. **86**, 1877 (2001).
[19] H. Kotegawa, K. Ishida, Y. Kitaoka, T. Muranaka, and J. Akimitsu, Phys. Rev. Lett. **87**, 127001 (2001).
[20] Y. Kong, O. V. Dolgov, O. Jepsen, and O. K. Andersen, Phys. Rev. B **64**, 020501(R) (2001).
[21] J. Kortus, I. I. Mazin, K. D. Belashchenko, V. P. Antropov, and L. L. Boyer, Phys. Rev. Lett. **86**, 4656 (2001).
[22] J. M. An and W. E. Pickett, Phys. Rev. Lett. **86**, 4366 (2001).
[23] R. Yu and P. K. Lam, Phys. Rev. B **37**, 8730 (1988).
[24] M. Gupta, R. P. Gupta, and D. J. Singh, Phys. Rev. Lett. **95**, 056403 (2005).
[25] A. Aguayo and D. J. Singh, Phys. Rev. B **69**, 155103 (2004).
[26] D. J. Singh and L. Nordstrom, *Planewaves, Pseudopotentials and the LAPW Method*, 2nd ed. (Springer, Berlin, 2006).
[27] D. Singh, Phys. Rev. B **43**, 6388 (1991).
[28] D. J. Singh, M. Gupta, and R. Gupta, Phys. Rev. B **75**, 035103 (2007).
[29] F. Gingl, T. Vogt, and E. Akiba, J. Alloys Compd. **306**, 127 (2000).
[30] One of the difficulties with using hydrides to store hydrogen for vehicles is that ordinarily, a heat of formation for the hydride of ~ -40 kJ/mol H_2 is needed because of the requirement for equilibrium with H_2 gas near ambient conditions. This is a substantial value that poses severe engineering challenges for refueling and represents a large energy that is lost to the transportation application. This requirement of ~ -40 kJ/mol H_2 would be relaxed for hydrides that either develop very soft lattices upon hydriding or where H has very low vibrational frequencies. The ideal hydride, which would be a material that is in thermodynamic balance with H_2 gas at ambient conditions and has zero heat of formation, would require an almost certainly unobtainable H effective Einstein frequency of 34 cm^{-1} at ambient temperature. However, a hydride with a H effective Einstein frequency of 135 cm^{-1} would be in the desired equilibrium with only half the heat of formation of a normally stiff hydride. A 135 cm^{-1} Einstein frequency would imply a H rms displacement of ~ 0.7 Å at ambient conditions, which may be possible in, e.g., complex ionic hydrides, and it may be that some fraction of the entropy could come from softening of the host lattice, which would make the situation more favorable. It is, therefore, of interest to consider mechanisms for obtaining very soft H phonons in hydrides.
[31] These energies include relaxation of the internal structural coordinates in the cell. However, the relaxation energies are small for these high symmetry, small unit cell structures. Relaxation energies may be higher for more realistic patterns of H positions.
[32] The high temperature spectrum shows a quadrupole splitting of 1 kHz, corresponding to an EFG of $\sim 2.0 \times 10^{19}$ V/m^2, while below 145 K, the shoulders are at a splitting of 10 kHz, or an inferred EFG of $\sim 2.0 \times 10^{20}$ V/m^2; V. G. Kodibagkar and M. S. Conradi (private communication).
[33] A. Kokalj, J. Mol. Graphics Modell. **17**, 176 (1999); code from http://www.xcrysden.org